Supplemental Figures for "Long-Term Monitoring of Cloud Water Chemistry at Whiteface Mountain: The Emergence of New Chemical Regime"

Section 1. Fraction of Measured Organic Carbon that is Water Soluble

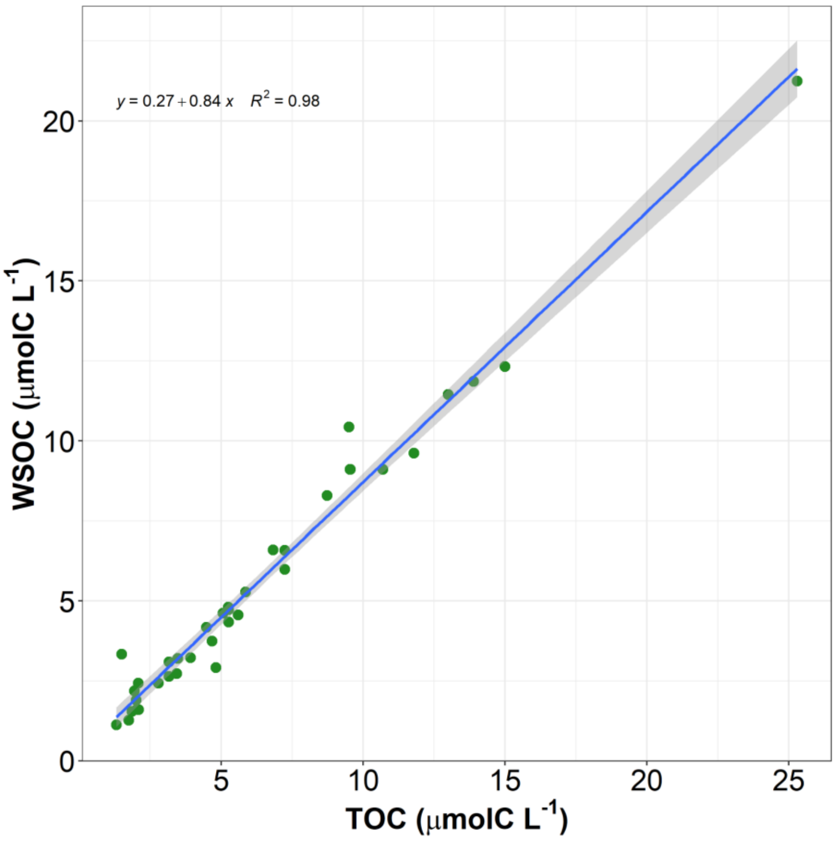

Figure S1. Measured Water Soluble Organic Carbon (WSOC) concentrations vs measured Total Organic Carbon (TOC) concentrations 38 WFM cloud samples collected in 2018 and 2019 where these measurements were obtained. WSOC is consistently 80-90% of TOC, with an average of 84%. The slope of the regression line is determined by an ordinary least squares regression.

Section 2. Calculating an average cloud LWC for each cloud water sample

An average LWC was recorded in the long-term cloud water dataset for each bulk cloud water sample. However, the details behind how this value was determined were not recorded. There is some indication that these average LWC values were calculated by including all LWC values >= 0.05 g m^{-3}. However, This calculation may lead to a high bias by including rain events, during which the collector was not actually deployed. To ensure that LWC values measured during rain events aren't included in the LWC averaging, we recalculate the average LWC from 2009 to 2021 based on the available hourly meteorology data. The cloud water data prior to 2009 does not include when the collector was deployed, making measurements prior to 2009 subject to greater uncertainty. In our recalculation, hourly LWC values were only included in the 3 or 12 hour average if: 1) LWC $\geq$0.05 g m^{-3}, 2) the cloud water collector was deployed > 25% of the time and 3) rain was detected < 15% of the time.

The performance of this algorithm was tested using 1-minute resolution data available for the 2016 collection season. Figure S2 compares the recalculated average LWC values to the average LWC determined from the 1-minute resolution LWC data for every minute the cloud collector was deployed. This demonstrates that accounting for deployment time and rain detection reduces bias and random error of the LWC values. Recalculated average LWC values that follow the criteria above are colored red, while blue data points represent the cloud water samples that would be excluded from the CWL. Using this methodology, approximately 29% of cloud water samples are removed from analysis due to the inclusion LWC values while the collector was not deployed.

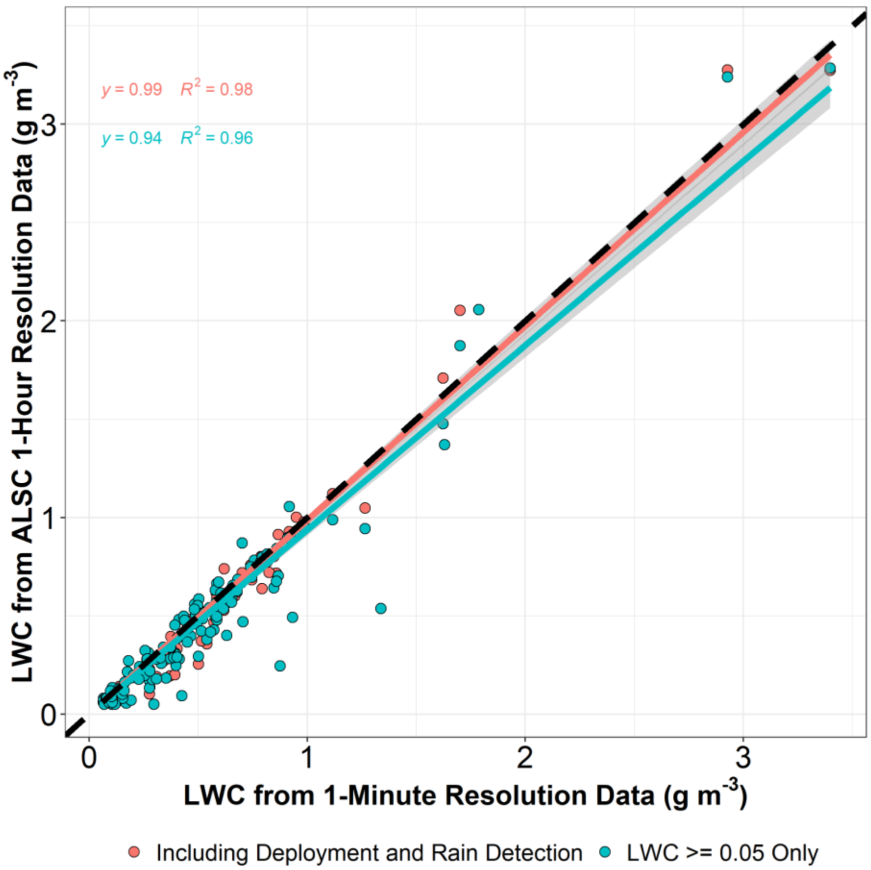

Figure S2. 12 hourly averaged LWC recalculated based on the hourly LWC data reported by ALSC in 2016 vs 12 hourly averaged LWC calculated based on 1-minute LWC measurements only when the cloud water collector was deployed. Blue points represent LWC averages when LWC > 0.05 g m^{-3} while the red points represent LWC averages when all conditions of:LWC > 0.05 g m^{-3}, the cloud collector is deployed for > 25% of the time, and rain is detected < 15% of the time are met. When accounting for time when the cloud water collector isn't deployed in addition to LWC improves the relationship between the ALSC reported LWC and minute resolution LWC.

In addition, LWC values with values above 2 g m^{-3} were not included in the LWC$_{samp}$ calculation based on the reasonable assumption of rain.

a) Theil-Sen Slope and Mann Kendall P-Value Valid Dataset

Analyte	*Slope*	*P-Value*
pH (units/yr)	0.0514	$p < 0.001$
Conductivity (uS/cm yr)	-2.2863	$p < 0.001$
SO4 (ueq/L yr)	-5.1386	$p < 0.001$
NO3 (ueq/L yr)	-1.7642	$p < 0.001$
NH4 (ueq/L)	-2.0083	$p < 0.001$
TOC (umolC/L yr)	9.2176	$p < 0.001$
Ca (ueq/L yr)	0.1389	0.199
Mg (ueq/L yr)	0.0272	0.172
K (ueq/L yr)	-0.0009	0.906
Na (ueq/L yr)	-0.0187	0.259
Cl (ueq/L yr)	-0.0956	0.00267

b) Theil-Sen Slope and Mann Kendall P-Value Complete Dataset

Analyte	*Slope*	*P-Value*
pH (units/yr)	0.0547	$p < 0.001$
Conductivity (uS/cm yr)	-1.9741	$p < 0.001$
SO4 (ueq/L yr)	-4.1326	$p < 0.001$
NO3 (ueq/L yr)	-1.3485	$p < 0.001$
NH4 (ueq/L)	-1.2964	0.00603
TOC (umolC/L yr)	22.4134	$p < 0.001$
Ca (ueq/L yr)	0.4947	$p < 0.001$
Mg (ueq/L yr)	0.1174	0.00126
K (ueq/L yr)	0.0198	0.0819
Na (ueq/L yr)	0.0050	0.782
Cl (ueq/L yr)	-0.0553	0.0313

Table S1: Theil-Sen regression slopes and associated Mann-Kendall test p-values for the a) valid and b) complete cloud water datatsets.

Section 3. Comparing "Valid" versus "Invalid" data sets

Another consideration for assessing measurement validity based on ion balance criteria alone is that complete chemical analysis requires a minimum volume of water (typically 250mL). If a given analyte could not be measured due to inadequate sample volume, the sample would be considered "Invalid" by default simply because ion balance could not be assessed. This protocol resulted in observational bias for samples where sufficient cloud water was collected for full analysis, which typically correspond to clouds with higher liquid water content (LWC) and/or longer collection intervals.

Across all years, annual median LWC is higher within the "Valid" data set. Higher LWC tends to correspond to more dilute samples, thereby reducing concentrations (Aleksic et al., 2010). Changes in LWC, however, do not explain the divergence in analyte concentrations starting around 2006 between the "Valid" and "Invalid" data sets since the LWC trends do not diverge and instead remain relatively unchanged.

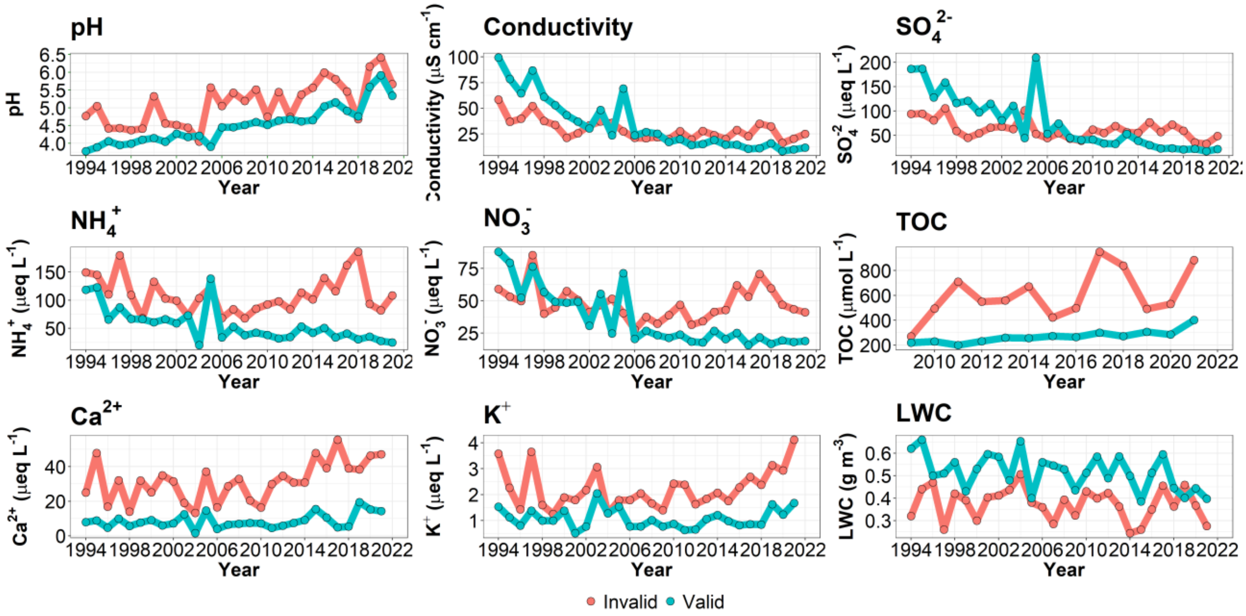

Figure S3. Comparisons between the “Valid” and “Invalid” data sets for annual median concentrations of six analytes of interest, conductivity, pH and LWC.

Some analytical laboratories handle data quality control differently, for example by repeating measurements when ion balance for a sample is not attained, and nevertheless classifying the data for that sample as valid if the subsequent measurements match the initial measurements. Unfortunately, retesting the old cloud water samples collected at WFM is not possible, as the samples have not been archived, and repeat testing would again skew the statistics toward samples with greater volume of collected cloud water (since repeat testing would not have been possible for the lowest volume samples).

Section 4. Impact of LWC on total ion content and total organic carbon concentrations

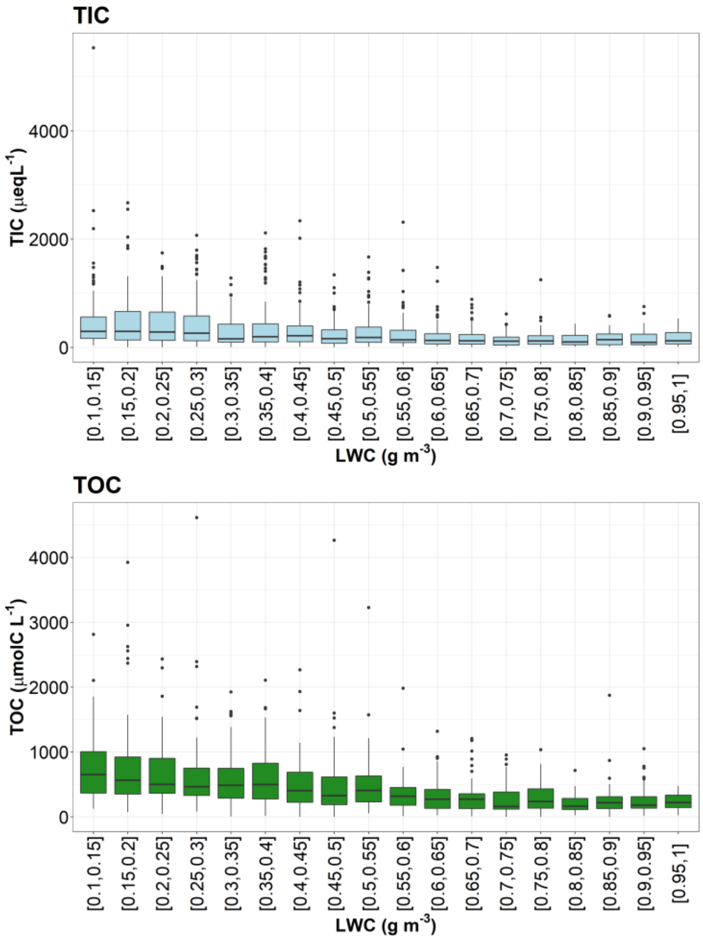

Figure S4. Total Ion Concentration (TIC) and TOC concentrations vs LWC using a similar binning procedure as described in Alesik et al 2009. With the exception of the lowest LWC bins, there is a general decrease in TIC and TOC concentrations as LWC increases. Within each LWC bin, there is considerable variability.

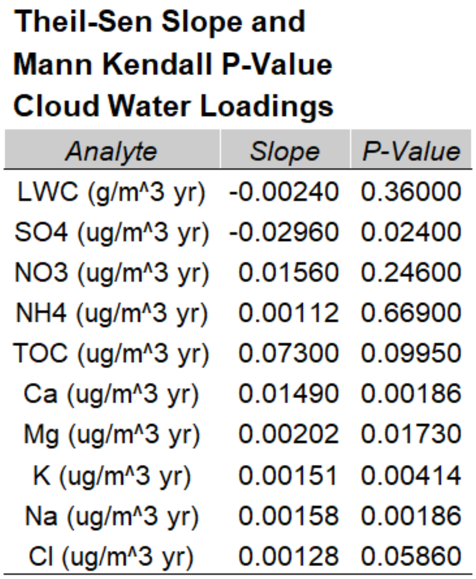

Theil-Sen Slope and Mann Kendall P-Value Cloud Water Loadings

Analyte	*Slope*	*P-Value*
LWC (g/m^3 yr)	-0.00240	0.36000
SO4 (ug/m^3 yr)	-0.02960	0.02400
NO3 (ug/m^3 yr)	0.01560	0.24600
NH4 (ug/m^3 yr)	0.00112	0.66900
TOC (ug/m^3 yr)	0.07300	0.09950
Ca (ug/m^3 yr)	0.01490	0.00186
Mg (ug/m^3 yr)	0.00202	0.01730
K (ug/m^3 yr)	0.00151	0.00414
Na (ug/m^3 yr)	0.00158	0.00186
Cl (ug/m^3 yr)	0.00128	0.05860

Table S2. Theil-Sen regression slope and associated Mann-Kendall p-values for cloud water loadings for the years 2009-2021.

Section 5. Two independent measures suggesting missing analytes are pH dependent

The ratio of measured cations to measured anions tends to increase with measured pH for all years of the study (Figure S5), and nearly all samples exhibit more measured cations than anions for pH≥5.5. As noted in the manuscript, greater measured cations than anions suggests that there are anions present in solution that are not being measured with the current suite of instruments. Within the past decade, the Cation/Anion ratio was almost always > 1, even at pH as low as 3.5. Many of the older samples also exhibited Cation/Anion ratios as high as 3 at pH of 5. The cation and anion concentrations versus pH are further explored in Figure S6 and S8.

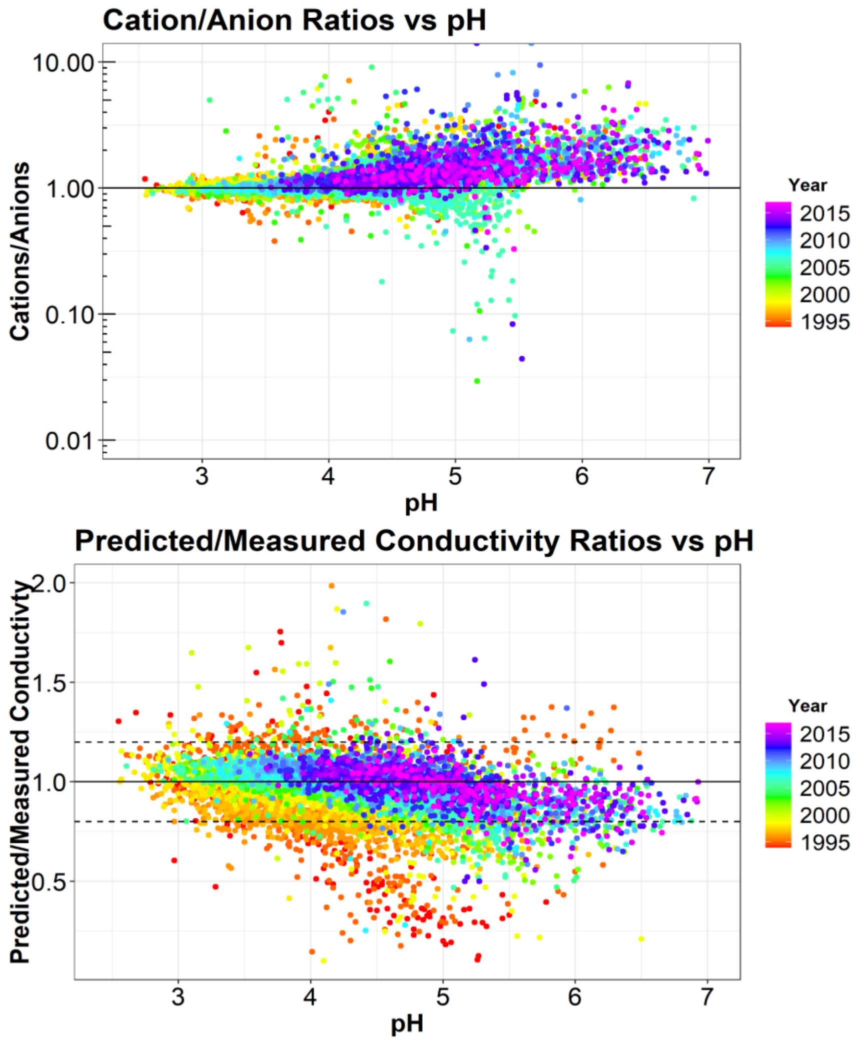

Figure S5. Cation/Anion ratio versus pH (top) and Predicted/Measured Conductivity vs pH (bottom) colored by the year the sample was collected, for all cloud water samples from 1994-2017. The dotted lines show 20% uncertainty in Predicted/Measured conductivity.

Also shown in Figure S5 is the ratio of predicted conductivity to measured conductivity versus pH. Predicted conductivity is calculated using the concentrations of measured cations and anions and their associated limiting molar conductivities. The first few years of data shows greater variability both above and below predicted/measured conductivity of 1, suggesting that the conductivity measurement uncertainties were higher in the earliest years of the cloud water collection program. Note that since at least 2006, nearly all samples with pH > 5.5 exhibited higher measured conductivity than predicted from the measured analytes. Systematic underprediction of the measured conductivity suggests the presence of ions that are not being measured. On the contrary, samples with pH < 4 tended to exhibit lower conductivity than predicted from the measured analytes, especially in recent years. Overprediction of conductivity might be due to the presence of organic molecules like sugars and starches that can lower the conductivity of a salt solution (Kaewthong and Wattanachant, 2018). This potential effect could be dampening the impact of missing analytes on the underprediction of conductivity at high pH.

Section 6. Potential impact of bicarbonate ion concentrations on ion imbalance

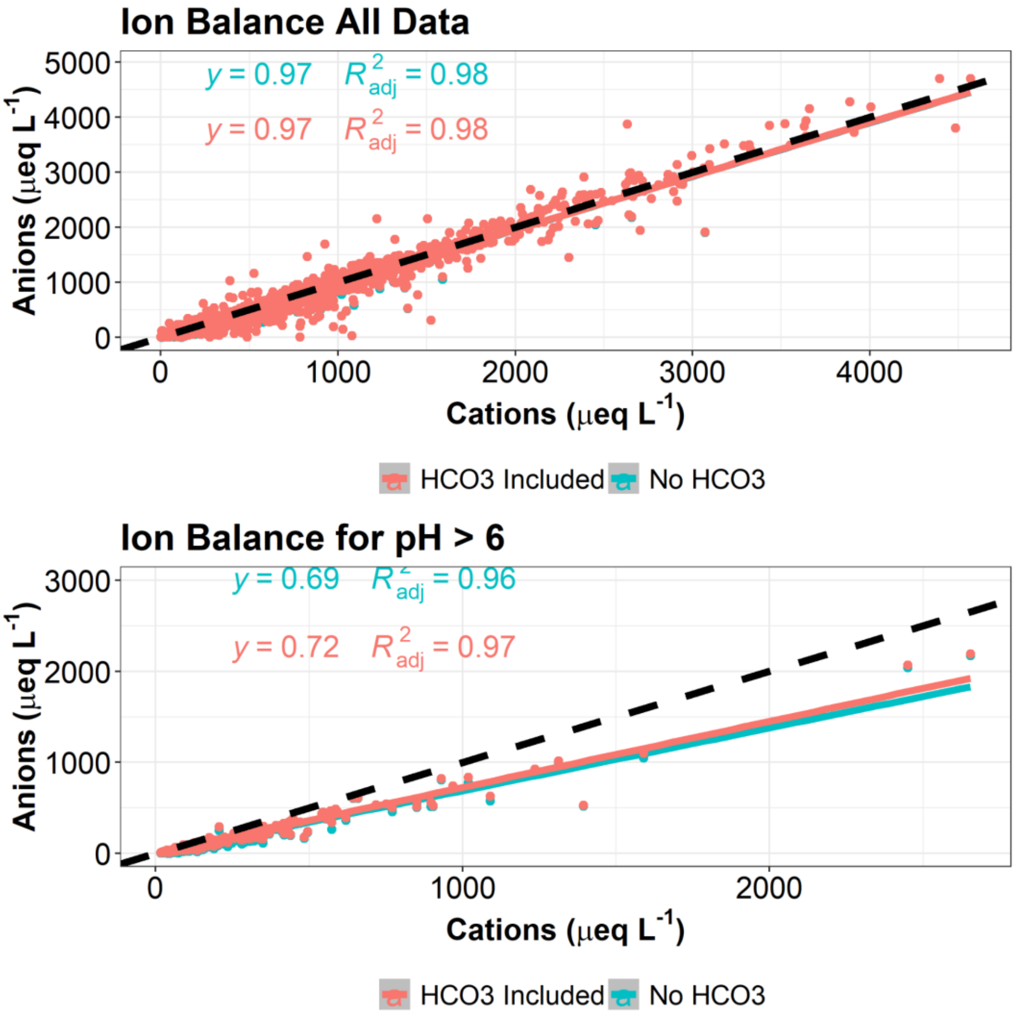

Figure S6. Anions vs Cations when including HCO_3^- within the ion balance for the entire dataset (top) and for samples that have measured bulk cloud water pH values > 6 (bottom). There are virtually no changes in ion balance for the vast majority of samples, but for pH values > 6 HCO_3^- there is a slight impact.

Section 7. Another Relationship with Ion Imbalance: TOC

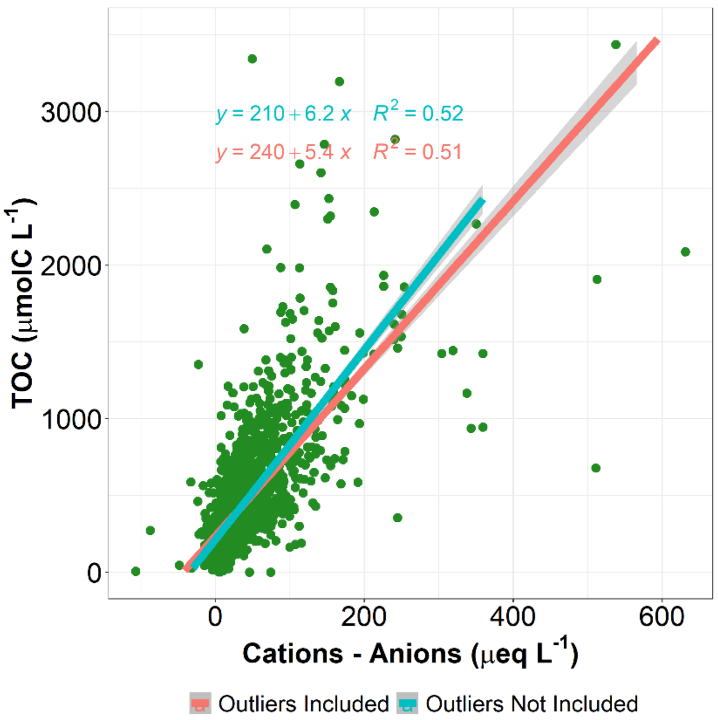

Figure S7. Measured TOC concentrations versus Ion Imbalance, i.e. Cations - Anions, for all cloud water samples from 2009 to 2021. Regression lines are calculated using ordinary least squares regression. A strong positive relationship between TOC and ion imbalance suggests that unmeasured organic compounds are a significant contributor to ion balance. There are 4 outliers within the TOC measurements that could lead to a low bias in the slope of the regression. To account for this, regression lines were calculated include and excluded the outliers. The inclusion of the outliers led to a slightly decreased slope, and had virtually no change in the R^2 value, indicating that the outliers had little impact on the regression line.

Section 8. Ion balance analyzed by pH bins

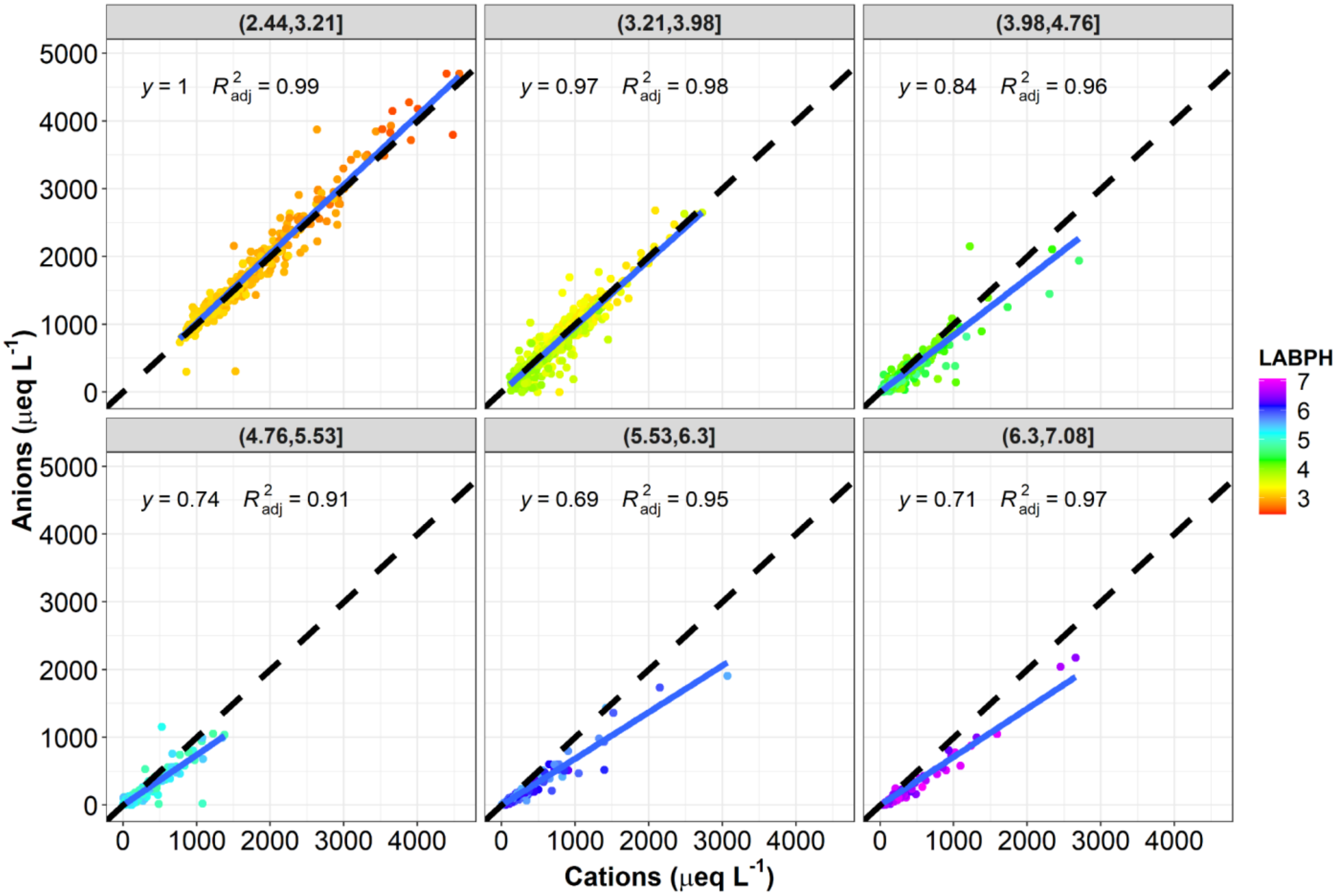

Figure S8. Anions vs Cations, split into 6 pH bins for Valid and Invalid cloud water samples collected from 1994-2021. As pH increases, there is a clear drop in the slope of the line. The largest decreases in slope occur in the bin of 3.98-4.76 and 4.76-5.53, which coincides with the pKas of formic and acetic acid (3.74 and 4.75 respectively), the two most common organic acids for in cloud water samples. As the pH increases, the fraction of these acids that are in their anionic forms increases. The increasing ion imbalance as pH increases could be evidence of greater fraction of organic acids existing in their ionic form, thus contributing to a growing ion imbalance.

Section 9. Size-resolved Aerosol Composition

Aerosol composition as a function of dry particle size is needed to better interpret the cloud water dataset. Since this information is not currently available from the summit of WFM, nor was this information available when the long-term cloud water data set was obtained, we looked for size resolved aerosol composition measurements conducted within the region. Measurements conducted mostly in Toronto, Ontario were referenced several times in the paper, as they show both the base cation mass distributions and organic acid mass distributions with respect to the dry aerosol size (VandenBoer et al., 2011). These measurements were obtained during the measurement period of the current study. This dataset was re-evaluated for our specific purposes.

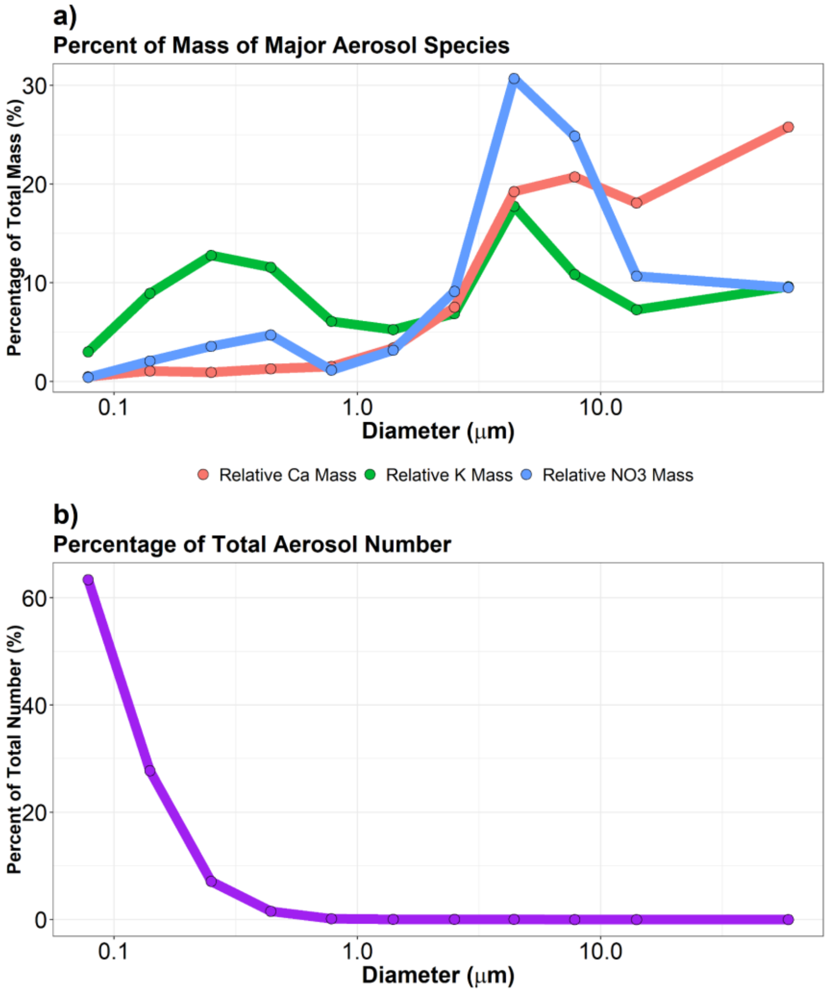

Figure S9. a) Normalized mass distributions of Ca^{2+} (red), NO_3^- (blue) and K^+ (green) as a function of particle diameter based on measurements in Toronto, Dorset, Lambton Shores, and Egbert in 2009 (VandenBoer et al., 2010). These observations show that the vast majority of Ca^{2+} mass is contained in aerosol with diameters > 1 µm, while K^+ exhibits a bimodal distribution, with significant proportions of mass contained in diameters above and below 1 µm. NO_3^- is also largely contained in aerosol with diameters > 1 µm in the plot above, but with substantial variability sample to sample. b) Calculated percent of total aerosol number as a function of particle diameter, based on the total measured aerosol mass and an estimate for the particle density.

Section 10. Measured and Estimated Cloud Droplet pH versus LWC, NH_4^+ and NO_3^-

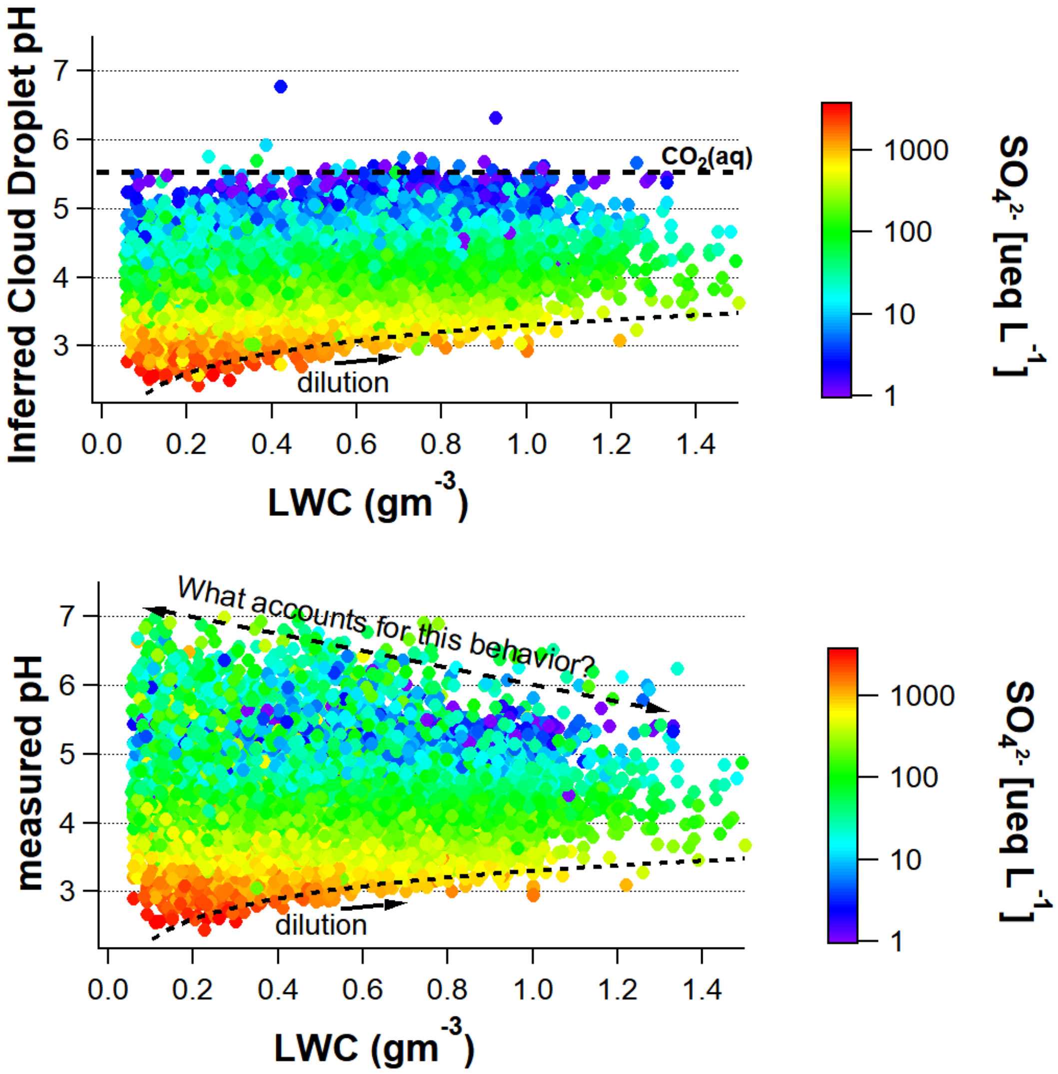

Figure S10. a) Measured bulk cloud water pH, and b) estimated cloud droplet pH as a function of the reported average Liquid Water Content (LWC) for all cloud water samples from 1994 to 2021, colored by measured sulfate concentrations.

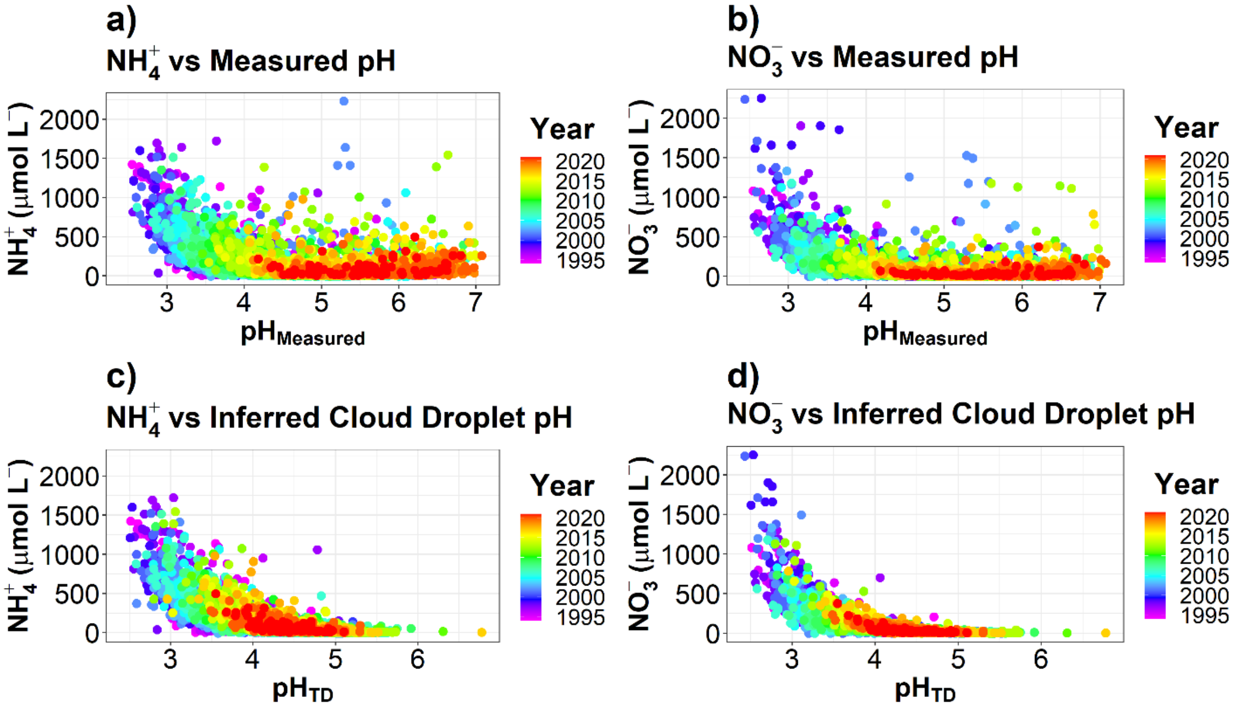

Figure S11. Measured NH_4^+ and NO_3^- concentrations versus a) and b) bulk cloud water pH, and c and d) drop pH. Similar to TOC, the relationship between NH_4^+ and NO_3^- and pH is simplified when accounting for the influence coarse mode aerosol, with increasing concentrations of both analytes associated with lower drop pH.

Section 11. Wildfire Smoke Influence at Whiteface Mountain

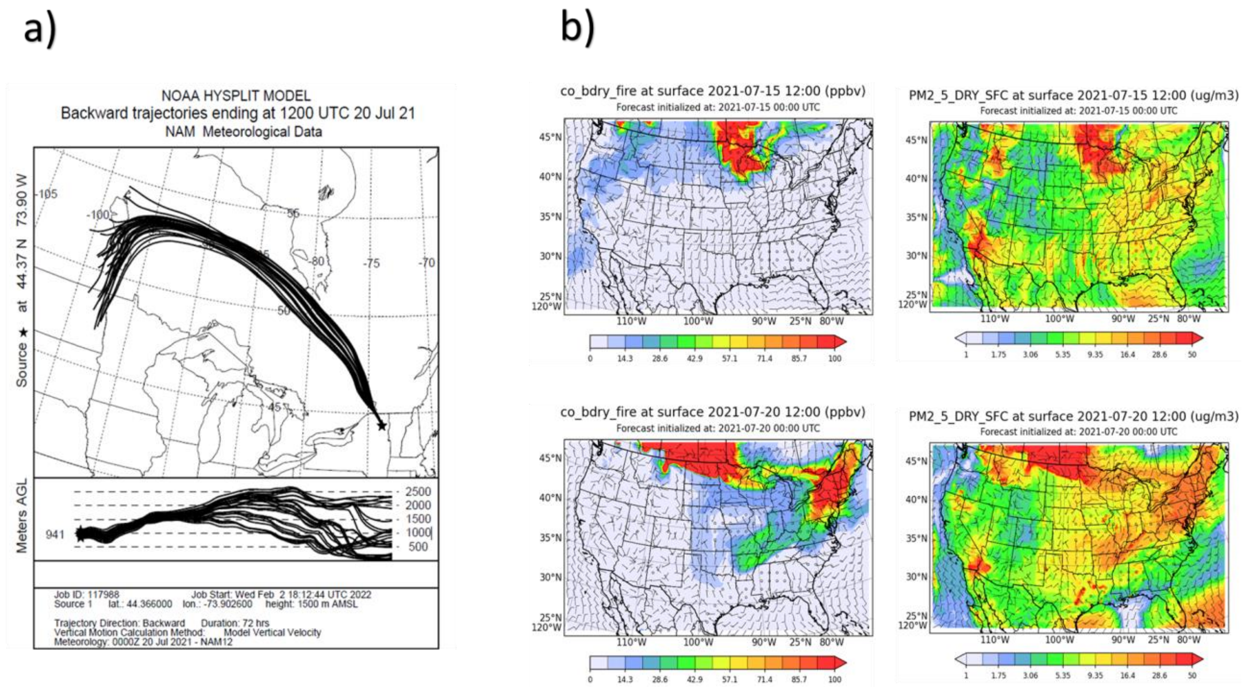

Figure S12. a) 5 day ensemble HYSPLIT back-trajectories using North American Mesoscale (NAM) 12 meteorological data launched on July 20th, 2021 at 12:00 UTC. b) WRF-Chem Forecast of carbon monoxide (CO) from boundary layer fires and surface PM 2.5 on July 15th, 2021 and on July 20th, 2021. A clear source of wildfire smoke emissions over Manitoba, Canada occurred on July 15th that eventually impacted air quality in New York on July 20th.